Manufacturing and preliminary space assessment of a European source of 8-channel silicon photodiodes for optical encoders

Authors: M. Bregoli[(1)*], S. Ceriani[(1)], M. Erspan[(1)], A. Collini[(2)], F. Ficorella[(2)], L. S. How[(3)]

[(1)]*Optoelettronica Italia Srl (Optoi), Via Vienna 8, 38121 Gardolo (TN), Italy*

[(2)]*Fondazione Bruno Kessler (FBK), Via Sommarive 18, 38123 Povo (TN), Italy*

[(3)]*AdvEOTec, 6-8 Rue de la Closerie, Lisses - ZAC Clos aux Pois, 91052 Evry Cedex, France*

Abstract

This paper presents recent results on the preliminary space assessment of a European source of photodiode arrays. The device under study is a monolithic silicon photodiode array composed of 8 independent channels, developed by Optoi through an ESA contract, as part of the Technology Research Programme (TRP). The activities of design, manufacturing, preliminary evaluation and preliminary radiation testing were carried out since the beginning of 2014 till late 2015.

Keywords: photodiodes, optical encoders, full hermeticity

I. INTRODUCTION

The device presented in this paper is a monolithic silicon photodiode array, composed of 8 independent channels (Figure 1) and representing the future receiver to be used within Codechamp optical encoders that are deployed inside spacecraft Space Mechanisms. The reference device currently used within these systems is based on phototransistor technology and it has been the object of previous developments [1][2][3][4]; the choice of a photodiode device provides various advantages if compared to the phototransistor counterpart, in terms of speed, radiation hardness and component robustness.

Such development represents Optoi's latest involvement in the space field, following several projects funded by CNES, ESA and ASI, based on similar devices and technologies [5].

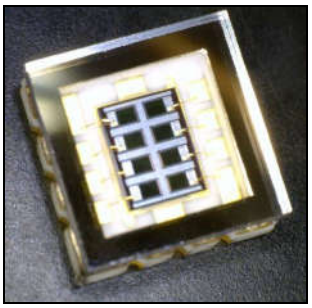

Figure 1: assembled device

II. DEVICE DESIGN AND MANUFACTURING

The die measures about 2.30 x 1.66 x 0.30mm^3 (L x W x T). The package is a ceramic LCC (Leadless Chip Carrier) with gold plated terminations measuring 4.57 x 4.57 x 1.14mm^3. The microelectronic assembled package is closed with an optical borosilicate glass lid measuring 4.50 x 4.50 x 0.55mm^3.

In this project, different device variants have been designed and manufactured, in order to compare them in terms of functionality and robustness. The nature of the device's anti-reflective coating represented one of these variants.

The manufacturing process has been optimized from previous runs of similar devices for space and industrial applications [5][6]. The fabrication of 6" silicon wafers has been carried out by FBK's Micro Nano Facility, in their class 10 front-end clean room, in close collaboration with Optoi. One specific split has been selected for the preliminary assessment programme, based on wafer-level measurements and functional validation on assembled devices; subsequently, a batch of around 100 devices was assembled, each with 8 channels connected.

The protective glass lid on top of the microelectronic ceramic package was brazed through eutectic process, representing a relevant improvement with respect to the more traditional gluing approach. Such advanced technology is meant to achieve higher degree of hermeticity and better control of the internal gas concentration, leading to a remarkable optimization in terms of robustness and reliability within the device build. In fact, the packaging solution making use of glued lid could be the origin of problems due to loss of hermeticity or high moisture content encountered in the past in some opto-parts, during on-ground testing within ESA projects.

Device traceability throughout the testing phase was possible by means of a two-digit / two-letter serial code marked by laser on the backside of the ceramic packages. In addition, as previously suggested by ESA die-level traceability was implemented, by marking every single die on wafer with numbers, indicating its exact position (coordinates) across the wafer itself.

[*]*Corresponding author. e-mail : research@optoi.com*

III. FUNCTIONAL VALIDATION

Electrical characteristics have been extrapolated by means of automated acquisitions on dedicated testing routines, in close collaboration with FBK. Table 1 reports a result overview related to a reference device.

Parameter	Unit	Average value	St. dev.
I fwd 0.5V	A	2.28E-05	6.36E-06
Idark 5V	A	-7.00E-12	2.26E-12
Idark 30V	A	-1.18E-11	3.49E-12
Cap 0V	F	2.13E-12	3.29E-14
Cap 5V	F	1.02E-12	3.00E-14
Rsh -10mV	Ohm	1.10E+10	6.58E+09
Rsh +10mV	Ohm	1.58E+09	4.76E+08

Table 1: electrical measurements on a reference device

The following response times have been measured: rise time *Tr* (10%-90%), fall time *Tf* (90%-10%), half-step rise time *Tr50%*, half-step fall time *Tf50%*. The recorded values are lower than 500ns for *Tr* and *Tf*, and lower than 250ns for *Tr50%* and *Tf50%*; it was evident that these measurement results are strongly dependent on the setup configuration. In fact, a wideband, high-speed current-feedback amplifier with a feedback resistance R=1MΩ was used for each channel readout, to comply with the reference circuit indicated by the end-user. It is to be noted that the dynamic response of the photodiode is intrinsically very small; this means that the output of the circuit mostly depends on the dynamic response of the opamp, which is much larger. Therefore this measure doesn't actually reveal the dynamic response of the photodiode itself, but rather the dynamic response of the whole system, depending on the chosen opamp.

Two types of electro-optical tests have been performed, with the device operating in photovoltaic mode (unbiased):

1. *Power Response*: a calibrated light source emitting at 850nm has been used to illuminate the device, and the photocurrent has been measured with different values of incident optical power, for verifying the photoresponse linearity
2. *Spectral Response*: the device has been illuminated at different wavelengths (selected by means of a monochromator), and the photocurrent has been measured. A typical trend is shown in Figure 2. Inter-channel variation can thus be extrapolated for the wavelength range of interest (a typical value lower than 10% was recorded on the device shown in Figure 2, at 850nm ±30nm)

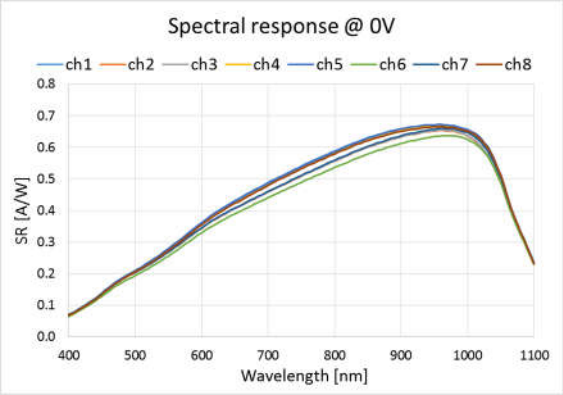

Figure 2: spectral response on a reference device

IV. PRELIMINARY EVALUATION TESTING

The preliminary evaluation test plan (P-ETP) was defined through technical discussion with AdvEOTec and ESA. Its agreed release, involving a total number of about 40 devices (each with 8 channels connected) is shown in Figure A. 1 (see Appendix). Such P-ETP was actually extracted from a more extended ETP, which was issued in the course of the project activity based on ESCC 226500 and keeping into account GR468 Core Issue 2.

All the parts submitted to the pre-evaluation testing have been initially subjected to successful fine and gross leak tests, following MIL-STD-883 M1014.13. Some unlidded devices were intentionally included within the P-ETP, together with the nominal (lidded) ones, in order to evaluate the intrinsic characteristics of the die itself and verify the impact of the assembly on the device reliability.

The preliminary evaluation testing was conducted by AdvEOTec and it was mainly centred on the following parameters: photocurrent, dark current, shunt resistance, spectral responsivity, response linearity, capacitance, dynamics and optical cross-talk. Sometimes these measurements proved demanding in terms of resolution, accuracy and repeatability, and an initial phase of bench optimization and calibration was necessary, including direct comparison with the results generated by Optoi and FBK during the previous functional validation phase.

Temperature step-stress was carried out increasing temperature from 75 to 200degC by steps of 25degC. Results demonstrated that the fully assembled devices start degrading at 175degC (Figure 3). This test conducted on unlidded devices revealed that the die itself is very robust at high temperatures, up to 200degC, i.e. in line with the state of the art.

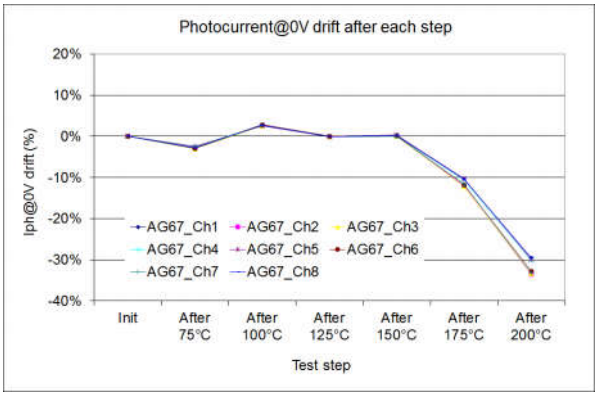

Figure 3: degradation in photocurrent during temperature step-stress

These results allowed the definition of the subsequent tests. Specifically, power step-stress was set at ambient temperature and the initial temperature for lifetest was set equal to 125degC.

Power step-stress, carried out increasing the applied reverse voltage from -5 to -40V for 48 hours at each step, showed no relevant drift in photocurrent or dark current.

The functional range determination was based on dark current and photocurrent, measured at different temperatures; Figure 4 shows photocurrent results.

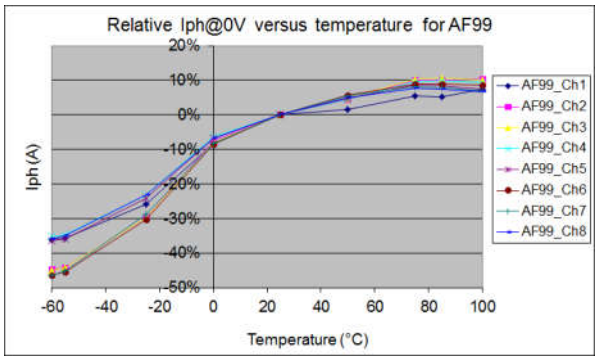

Figure 4: photocurrent variation as a function of temperature

Photocurrent linearity was verified by varying the incident optical power; over the whole measured range, the photoresponse is linear and fulfils the requirement originally expressed by the end-user, the linearity ratio remaining below 1.05 up to I_{ph}=1µA (Figure 5). This parameter indicates how the photoresponse curve bends with increasing optical power.

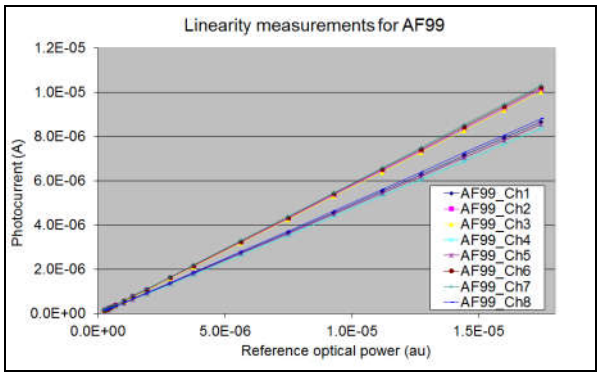

Figure 5: *linearity measurement (power response)*

After 100 temperature cycles between -55 and +125degC (transitions at 15degC/min and dwell time of 15mins), 8 tested devices didn't suffer from any relevant drift, except one channel of one device which was considered atypical in terms of dark current evolution; this particular channel had already presented anomalies in the I-V curve. It is believed that such initial anomaly in the I-V curve could be identified as a potential screening method for future batches. The other device parameters such as shunt resistance and photocurrent didn't show any relevant drift. Similar results have been obtained at 50degC. Linearity was not affected by temperature cycling, the linearity ratio remaining lower than 1.05, nor was the spectral responsivity; the capacitance remained within the reference requirement. The measurements of optical crosstalk after temperature cycling revealed that at -5V, the values between adjacent channels lay in the range between 21 and 36%. For such measurement, the optical spot was large about 50µm, on a motorized bench. No pin hole or shutter was used for this measurement. Similar results had been obtained before temperature cycling. It is believed that the measurement methodology affects the extrapolated result, on this specific test, and more representative results would be obtained using an optical shutter or a reticle. The tests of the device dynamics (after temperature cycling) confirmed to be strongly dependent on the setup. The primary contribution of each single channel was extrapolated through a measurement routine where each single active area was illuminated through a 50µm-large spot. When illuminating each single photodiode, the half-step response time was in the range of 400-500ns, i.e. compliant with the nominal requirements and in line with previous tests.

Lifetest was conducted at 125degC for the first 1000 hours. Since no relevant drift was observed, the test was continued at 150degC for another 1000 hours; such prolongation proved more aggressive. Despite the fact that dark current was not particularly affected, the measurements of shunt resistance and photocurrent showed that 2 devices out of 5 degraded more than the others (Figure 6).

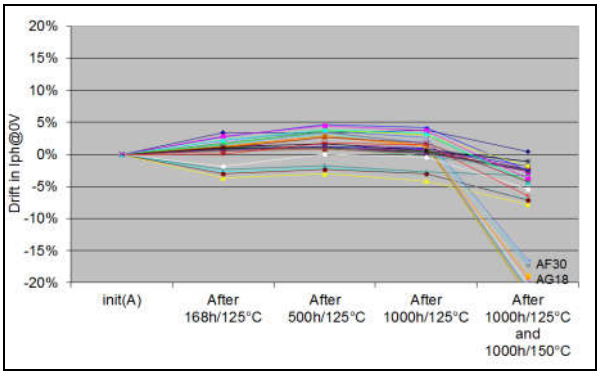

Figure 6: degradation of photocurrent on the second step of lifetest

Also linearity was affected by such harsh condition of lifetest: one of the two degraded devices mentioned above didn't satisfy the linearity requirement after the stress. On the other hand, another tested device belonging to the group of 3 with more limited degradation preserved its linearity.

At the end of the P-ETP testing phase some devices were submitted to physical analyses. Seven parts belonging to the temperature step stress and temperature cycling groups were subjected to a successful repetition of seal test. Besides, three unlidded devices belonging to the temperature cycling group were submitted to bond strength test; the bond strength measured after the 100 cycles proved robust, with a mean value above 10g on a total of 24 tested wires. Finally, Construction Analyses complemented the testing activity (Table 2). No major finding was raised, although a few observations were helpful for the optimization of the assembly methodology.

Inspection Requirement	Evaluation Criteria
External Visual	Mil. Std. 883J, Method 2009.11
Radiography	Mil. Std. 883J, Method 2012.9
Seal (Fine Leak Test)	Mil. Std. 883H, Method 1014.13 Condition A1
Seal (Gross Leak Test)	Mil. Std. 883J, Method 1014.14 Condition C1
PIND	Mil Std. 883J Method 2020.9 Condition A
Internal Gas Analysis	Mil. Std. 883J, Method 1018.7
Internal Visual Inspection	Mil. Std. 883J, Method 2013.1 & ESCC2045000
Bond Strength	Mil. Std. 883J, Method 2011.9 Condition D
Die Shear	Mil. Std. 883J, Method 2019.9

Table 2 : Construction Analyses

V. RADIATION STUDY

A radiation study was conducted in order to draw a basic figure of the developed technology hardness. Gamma ray irradiations have been conducted in ESTEC with a Co-60 source, at the dose rate of 36 rad(Si)/h, through progressive dose steps up to 47krad(Si) on both biased and unbiased devices (Table 3); proton irradiations have been conducted in UCL (Belgium), at 60 and 20MeV with two fluences per energy, on unbiased devices (Table 4). The main monitored parameters were namely the device dark current, the photocurrent and dynamics. Shortly after completion of the post-radiation tests, all devices have been subjected to ageing according to ESCC 22900, in order to analyze any possible recovery or further degradation.

Ionizing dose steps [krad(Si)]: biased and unbiased devices			
Dose rate = 36rad(Si)/h			
5	15	25	47

Table 3 : gamma radiation conditions

Proton fluences [p/cm^2] – unbiased devices			
Beam 1 = **60 MeV**		Beam 1 = **20 MeV** (degraded)	
5.5E+10	1.0E+11	2.0E+10	7.0E+10

Table 4 : proton radiation conditions

The analysis of the dark current degradation under gamma rays showed how its trend depends whether the device is biased or not during radiation. A more emphasized degradation has been recorded in the unbiased configuration than in the biased one (Figure 7 and Figure 8).

The degradation of the other electrical parameters was analyzed, considering capacitance, shunt resistance and breakdown voltage. No major degradation was noticed, neither under gamma nor proton radiation, however the drift of shunt resistance was analyzed in order to draw the device's nominal degradation figure.

In terms of photocurrent degradation, the developed technology proved robust according to the reference requirements, both under gamma rays and protons. Figure 9 shows the power response under gamma rays, whereas Figure 10 illustrates the spectral response under protons.

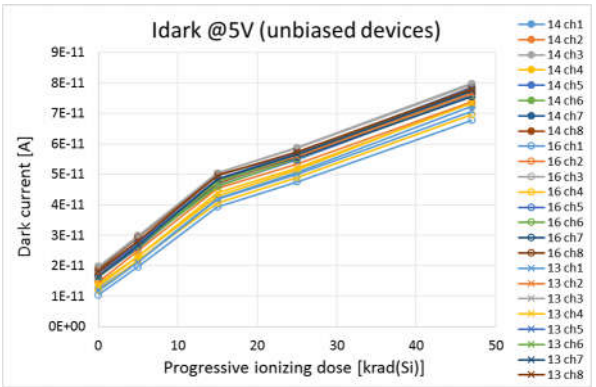

Figure 7: dark current degradation as a function of progressive ionizing dose, on devices unbiased during radiation

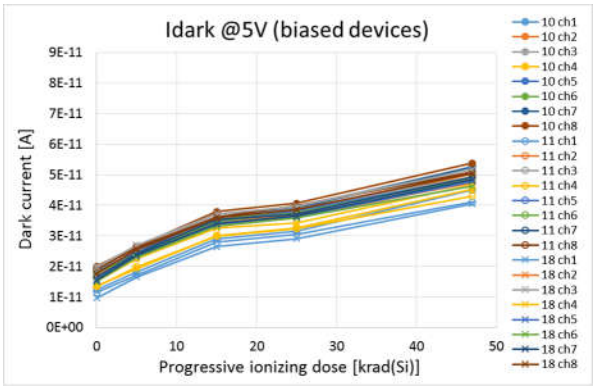

Figure 8: dark current degradation as a function of ionizing dose, on devices biased during radiation

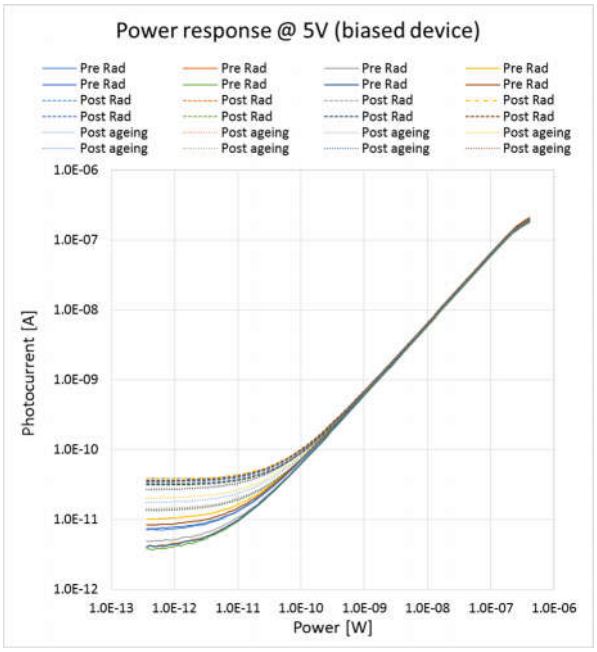

Figure 9: power response of a reference device biased during gamma irradiation up to 47krad(Si); in the range of interest, minimal variations were recorded i.e. lower than 2%

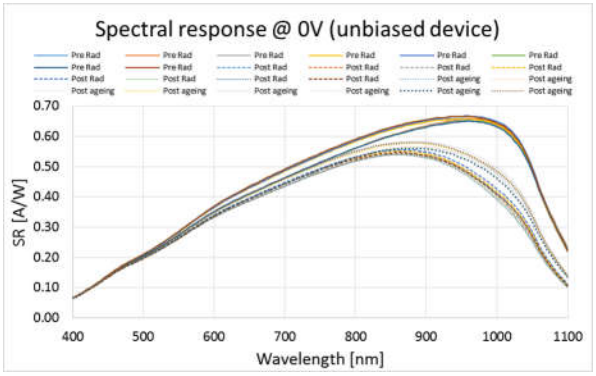

Figure 10: spectral response of one device unbiased during 60MeV-5.5E10p/cm^2 proton irradiation; comparison pre vs. post irradiation (degradation lower than -14%), and after ageing (lower than -12%)

In Figure 11, the photocurrent degradation observed at both proton energies is compared, based on the available results of power response. By using NIEL coefficients for silicon [7], it was possible to extrapolate the device degradation as a function of the displacement damage dose (Figure 12).

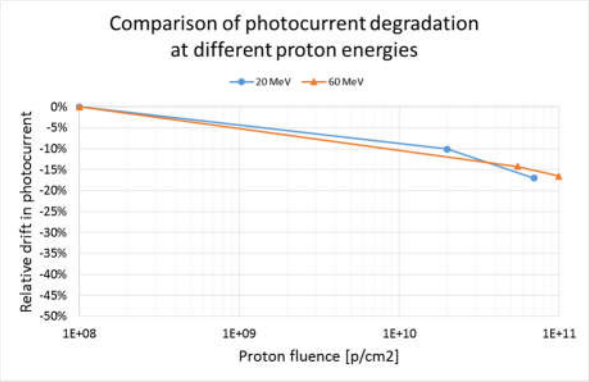

Figure 11: comparison of photocurrent degradation at 20 MeV and 60 MeV (averaged channels)

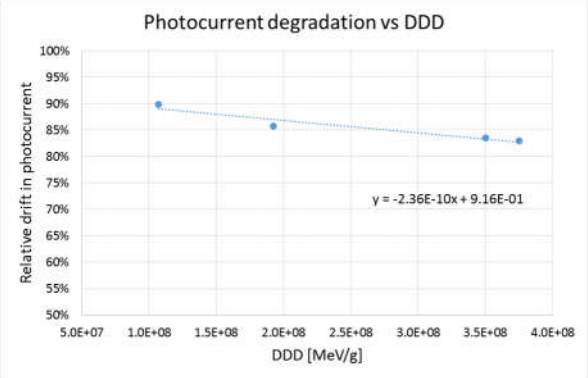

Figure 12: photocurrent degradation as a function of the DDD

The analysis of the dynamics showed that the devices were always within specification, both under gamma rays and protons.

In general, the ageing after gamma and proton radiation showed a slight recovery of the device characteristics, both electrical, i.e. dark current, and electro-optical, i.e. photocurrent.

CONCLUSION

This work summarizes the main outcome of a TRP activity, conducted for ESA and aimed at preliminarily assessing a new photodiode device for optical encoders to be used in space.

The activity allowed the determination of the device operative boundaries as well as the demonstration of its robustness, both under temperature stress and radiation.

All the results collected in the course of the preliminary evaluation testing have been taken into account for issuing the preliminary device datasheet, and drawing some considerations for a future device redesign.

ACKNOWLEDGMENT

The activity was funded by the European Space Agency, specifically in the framework of the Technology Research Program.

REFERENCES

[1] M. Bregoli, A. Maglione, M. Franceschi, A. Collini, P. Bellutti, P. Spezzigu, L. Bechou, "Customized and highly reliable 8-channel phototransistor array for aerospace optical encoders", *in Proc. ISROS Conf.*, 2009

[2] M. Bregoli, P. Bouvier, A. Maglione, "Microelectronic packaging assembly and qualification process flows of a customized phototransistor array for aerospace optical encoders", *in Proc. ISROS Conf.*, 2010

[3] M. Bregoli, C. Ress, L. S. How, A. Collini, "Space assessment program on a customized and highly reliable 8-channel phototransistor array for aerospace optical encoders", *in Proc ISROS Conf.,* 2012

[4] M. Bregoli, S. Ceriani, M. Erspan, A. Collini, F. Ficorella, G. Giacomini, P. Bellutti, L. S. How, S. Hernandez, K. Lundmark, "Development and ESCC evaluation of a monolithic silicon phototransistor array for optical encoders", *in Proc. ICSO Conf.*, 2014

[5] M. Bregoli, S. Ceriani, A. Collini, F. Ficorella, G. Giacomini, P. Bellutti, S. Hernandez, M. Zahir, K. Lundmark, "Recent achievements from a new European space optoelectronic component supplier", *in Proc. ISROS Conf.,* 2014

[6] Dalla Betta G. F., Pignatel G. U., Verzellesi G., Bellutti P., Boscardin M., Ferrario L., Maglione A., Zorzi N., "Design and optimization of an npn silicon bipolar phototransistor for optical position encoders". *Microelectronics Journal*, 1998, v. 28, n. 1, p. 45 – 54

[7] G.P. Summers, E.A. Burke, P. Shapiro, S.R. Messenger, R.J. Walters, "Damage correlations in semiconductors exposed to gamma, electron and proton radiations". *IEEE Trans Nucl Sci*, 40, No 6, pp1372-1379, 1993

APPENDIX

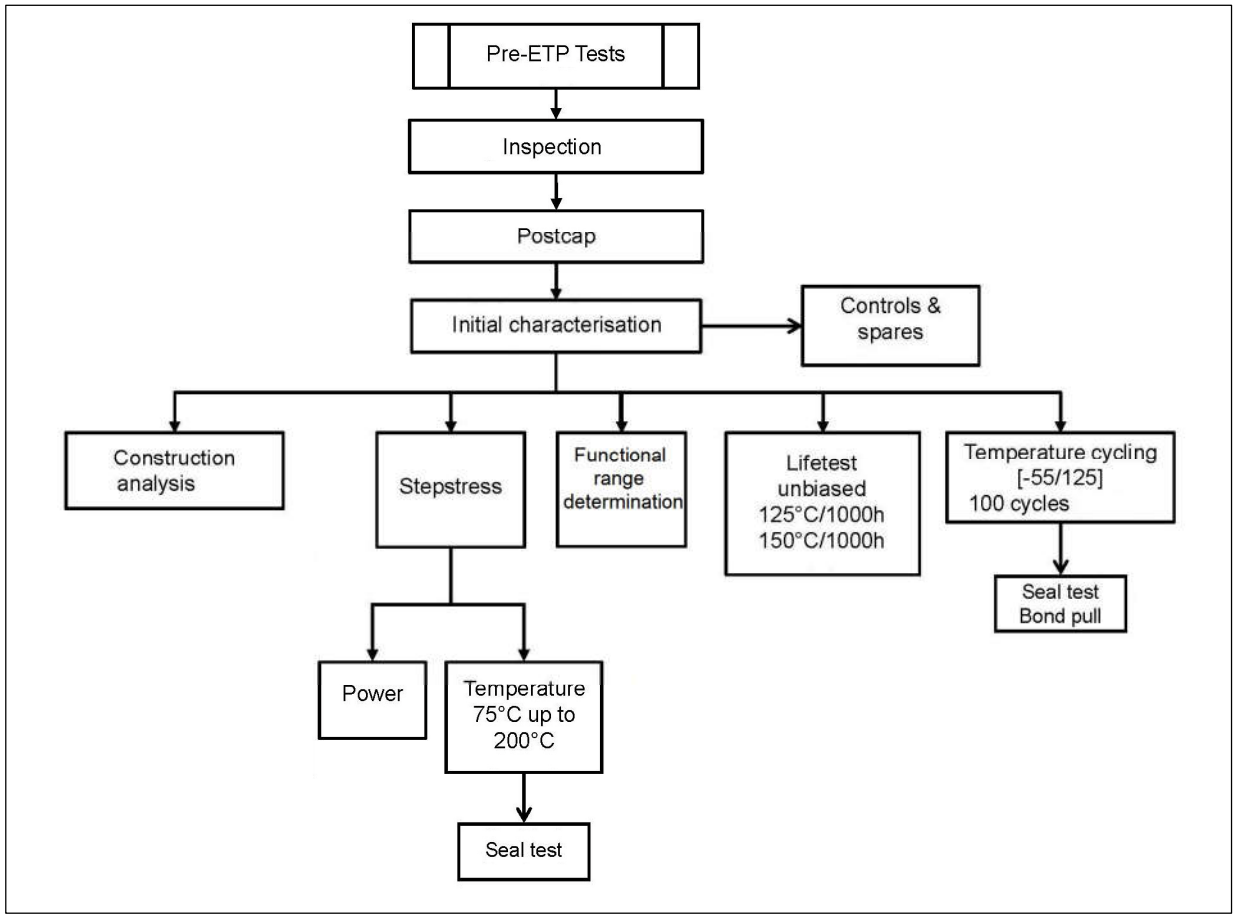

Figure A. 1 : *pre-evaluation test plan*